LETTERS

Protein kinase R reveals an evolutionary model for defeating viral mimicry

Nels C. Elde[1], Stephanie J. Child[2], Adam P. Geballe[2,3,4] & Harmit S. Malik[1]

Distinguishing self from non-self is a fundamental biological challenge. Many pathogens exploit the challenge of self discrimination by employing mimicry to subvert key cellular processes including the cell cycle, apoptosis and cytoskeletal dynamics[1–5]. Other mimics interfere with immunity[6,7]. Poxviruses encode K3L, a mimic of eIF2α, which is the substrate of protein kinase R (PKR), an important component of innate immunity in vertebrates[8,9]. The PKR–K3L interaction exemplifies the conundrum imposed by viral mimicry. To be effective, PKR must recognize a conserved substrate (eIF2α) while avoiding rapidly evolving substrate mimics such as K3L. Using the PKR–K3L system and a combination of phylogenetic and functional analyses, we uncover evolutionary strategies by which host proteins can overcome mimicry. We find that PKR has evolved under intense episodes of positive selection in primates. The ability of PKR to evade viral mimics is partly due to positive selection at sites most intimately involved in eIF2α recognition. We also find that adaptive changes on multiple surfaces of PKR produce combinations of substitutions that increase the odds of defeating mimicry. Thus, although it can seem that pathogens gain insurmountable advantages by mimicking cellular components, host factors such as PKR can compete in molecular 'arms races' with mimics because of evolutionary flexibility at protein interaction interfaces challenged by mimicry.

To counteract viral infections, PKR phosphorylates the translation initiation factor eIF2α in the presence of double-stranded RNA (dsRNA) from viruses[8,9]. This activity strongly inhibits protein synthesis and blocks the production of new virus particles. The crucial function of PKR in innate immunity is reflected by the evolution of numerous factors from various viruses that disable PKR to promote viral production[10], including a poxvirus-encoded mimic of eIF2α called K3L (Supplementary Fig. 1). Host proteins such as PKR, which interact directly with viral antagonists such as K3L, can be subject to molecular 'arms-races' in which amino-acid substitutions that directly affect interactions can be rapidly fixed by positive selection[11,12].

To determine whether PKR might be subject to positive selection, we cloned and sequenced complementary DNA of PKR from a panel of 20 primates representing more than 30 million years of evolutionary divergence. By considering ratios of the rates of non-synonymous (dN) and synonymous (dS) substitutions, we found evidence for ancient, episodic positive selection in primate lineages ($P < 0.0003$; Fig. 1a and Supplementary Table 1). In particular, one branch in Old World monkeys was calculated to have undergone 22 non-synonymous substitutions without any synonymous changes, one of the most intense episodes of positive selection reported for any primate gene (Supplementary Data). Likelihood ratio tests[13] using the entire phylogeny reveal that 17% of codons evolved with an average dN/dS ratio of 3.7, strongly supporting a finding of positive selection ($P < 0.0001$; Supplementary Tables 2 and 3), even after accounting for the potentially confounding effects of recombination and synonymous site variation[14] ($P < 0.0001$; Supplementary Tables 4 and 5). Positive selection is observed in each of the three domains of PKR—the dsRNA-binding domain, the spacer region and even the kinase domain—which is consistent with an extensive history of facing viral factors that directly bind PKR in these separate domains (Supplementary Fig. 1). Several residues in the kinase domain, which make direct contacts with eIF2α (ref. 15), are among the fastest-evolving residues in PKR (Fig. 1b and Supplementary Fig. 1), suggesting that selective pressure to evade eIF2α mimics may have driven changes in these residues.

Similarly, we find that positive selection has acted on the eIF2α mimic K3L (Supplementary Fig. 2). For instance, in a comparison of K3L from variola major (smallpox) and vaccinia viruses, we find a dN/dS ratio of 2.80 ($P < 0.001$), whereas fewer than 10% of orthologues in vaccinia and variola comparisons show any evidence of positive selection (average dN/dS = 0.10; N.C.E. and H.S.M., unpublished observations). This suggests that poxviral eIF2α mimics have also undergone positive selection and reflects the possibility that K3L has not achieved or maintained an optimal state of mimicry. Instead, K3L might continually evolve to counter adaptive changes in PKR.

In contrast with the rapid evolution of PKR, its substrate, eIF2α, is essentially unchanged in simian primates at the amino-acid level (dN/dS = 0 in a comparison of human and rhesus). Thus, PKR must recognize an unchanging substrate while evolving to discriminate against mimics such as K3L to be effective. If we consider that most viruses, including poxviruses[16,17], evolve at faster rates than primates, such challenges by mimics are daunting for hosts. Nevertheless, PKR can inhibit viruses encoding eIF2α mimics[10], suggesting that adaptive changes in PKR might help to overcome mimicry by these factors.

We investigated whether primate PKR orthologues differ in their ability to discriminate against K3L from vaccinia, the model poxvirus. Because the entire clade of extant poxviruses is very young relative to the divergence between primates[16,17], we could not investigate strict co-evolutionary dynamics between PKR and K3L. Instead, we used vaccinia K3L as a means to study the evolutionary strategies afforded PKR for counteracting substrate mimics that were faced over the course of primate evolution, which could leave PKR variants either susceptible or resistant to vaccinia K3L. Even though primate *PKR* alleles did not necessarily evolve under pressure from vaccinia K3L, our approach allowed us to identify the mechanisms by which host proteins might defeat mimicry more generally. Examining host–virus evolution from a similar perspective led to the identification of a region in the restriction factor Trim5α that confers specificity against ancient, extinct retroviruses but fails to protect humans from HIV[18,19].

A growth assay in yeast has provided a simple test of PKR function[20]. Human PKR recognizes and phosphorylates yeast eIF2α, as a result of its high level of similarity to primate eIF2α, to cause growth

[1]Division of Basic Sciences, [2]Division of Human Biology, and [3]Division of Clinical Research, Fred Hutchinson Cancer Research Center, Seattle, Washington 98109, USA. [4]Departments of Medicine and Microbiology, University of Washington, Seattle, Washington 98115, USA.

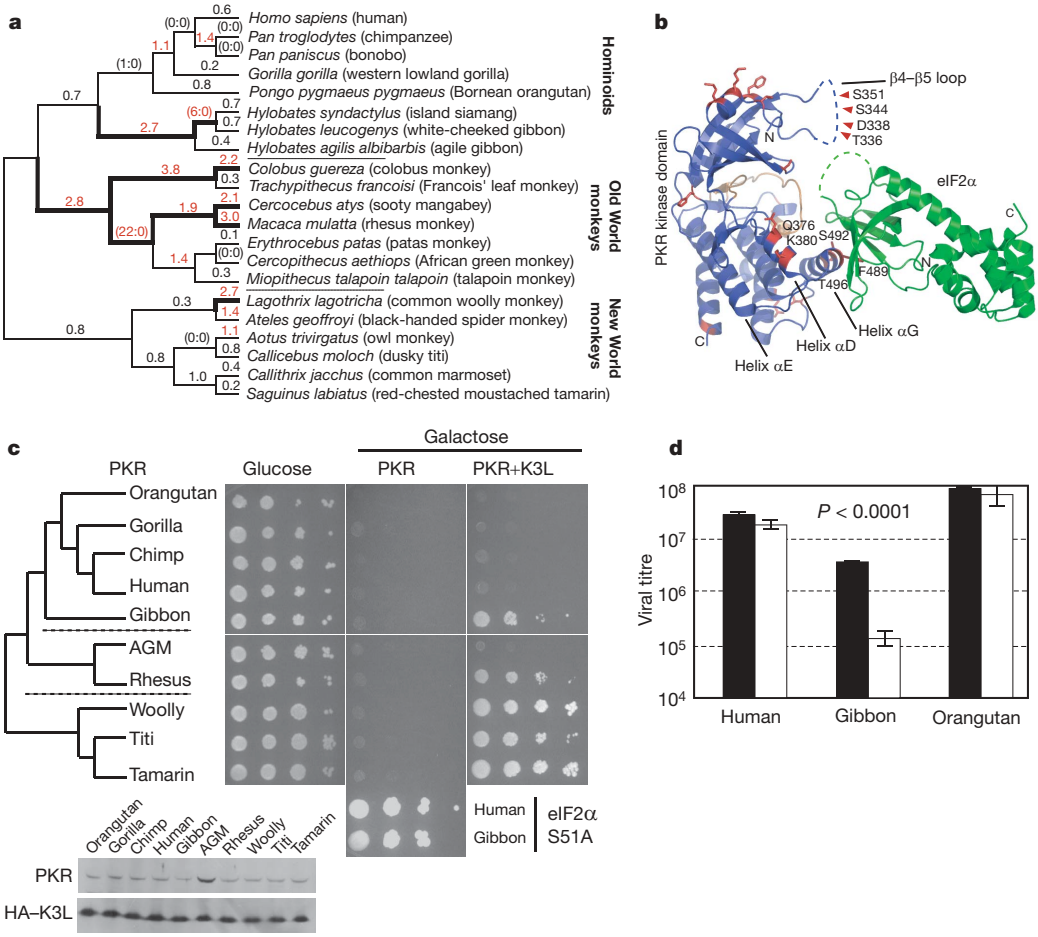

Figure 1 | Widespread positive selection has shaped PKR throughout primate evolution. **a**, *PKR* was sequenced from simian primates that together represent more than 30 million years of divergence. d*N*/d*S* values along each branch of the phylogeny are listed, and those with d*N*/d*S* > 1 are highlighted in red. Branches with bold lines, overlapping the set in red, indicate lineages found to be under positive selection by complementary model fitting analysis (see also Supplementary Table 6). Values in parentheses are shown for branches where no synonymous changes were observed ($S = 0$) and indicate the number of non-synonymous changes (N). **b**, Sites under positive selection (red) are mapped onto a ribbons representation of the complex of the PKR kinase domain (blue) with eIF2α (green) (PDB code 2A1A)[15]. The active site of PKR is shown in orange, and for technical reasons a large portion of the β4–β5 loop (dashed blue line) is invisible from the structure deduced from the co-crystal[15]. Residues under positive selection near the interface of PKR with eIF2α and K3L are noted in the β4–β5 loop (Thr 336, Asp 338, Ser 344, Ser 351) and the αD (Gln 376, Lys 380) and αG (Phe 489, Ser 492, Thr 496) helices. **c**, Plasmids encoding PKR variants from a panel of primates under pGal were introduced into yeast strains HM3 (eIF2α), HM2 (eIF2α and haemagglutinin (HA)-epitope-tagged vaccinia K3L) and J223 (eIF2α-S51A). Tenfold serial dilutions of transformants were spotted on plates containing either glucose or galactose (see Methods). Immunoblot analysis of PKR (top panel) and HA–K3L (bottom panel) is also shown (see Methods). For African green monkey (AGM), resistance to K3L might reflect differences in PKR expression in yeast. **d**, Primary fibroblasts from the indicated primates were infected in triplicate with wild-type (filled columns) or ΔK3L (open columns) vaccinia virus (multiplicity of infection 0.001). Virus production was assessed three days after infection by titring cell lysates. The significance of wild-type virus compared with ΔK3L is indicated (Student's *t*-test; error bars show s.d.). Minor variations of this experiment (not shown) revealed that ΔK3L infections typically produced about fivefold less virus than wild-type virus in gibbon cells.

arrest[15,21]. We expressed ten divergent primate *PKR* cDNAs in yeast to determine whether they differed in their ability to phosphorylate eIF2α. All primate *PKR* genes tested caused consistent levels of growth arrest, which specifically depended on phosphorylation of eIF2α (ref. 22) (Fig. 1c, middle). However, co-expression with vaccinia virus K3L uncovered marked differences in K3L inhibition of primate PKR orthologues, which leads to a rescue of growth[23] (Fig. 1c, right). *PKR* alleles from Old World and New World monkeys, and from white-cheeked gibbon, were generally quite susceptible to suppression of growth arrest by K3L from vaccinia and variola, whereas other hominoid *PKR* alleles showed only modest suppression by K3L (Fig. 1c and Supplementary Fig. 3). Thus, rapid evolution of primate PKR did not seem to alter eIF2α recognition significantly, but resulted in considerable differences in susceptibility to K3L. In particular, we find in the hominoid lineage that human, chimp, gorilla and orangutan PKR orthologues are 1,000-fold more resistant than gibbon PKR to growth rescue by K3L.

We further corroborated the large differences in K3L susceptibility uncovered by the yeast assay by infecting human, orangutan and gibbon fibroblast cell lines with either wild-type vaccinia virus or a strain with a *K3L* gene deletion (ΔK3L). Consistent with our yeast assays and previous reports in human cells[24] was our finding that ΔK3L virus had no significant effect on viral titre in human or orangutan cells but led to a substantial decrease in titre in gibbon cells (Fig. 1d). Vaccinia virus therefore depends on K3L for full infectivity in gibbon cells, where PKR is susceptible to K3L.

We wished to map critical genetic differences between 'resistant' and 'susceptible' *PKR* alleles to understand the basis of resistance to K3L. We first investigated helix αG of the kinase domain because residues 489, 492 and 496 have key functions in the recognition of eIF2α (ref. 15), yet they have evolved under recurrent positive selection (Figs 1b and 2). Whereas gibbon PKR (helix αG: Tyr 489–Ala 492–Thr 496 or Y-A-T) is susceptible to K3L in growth assays, the human αG configuration (F-S-T) in an otherwise gibbon PKR

backbone increases the resistance of gibbon PKR to vaccinia K3L (Fig. 2a, rows 1 and 2). In fact, the A492S substitution (Y-S-T) alone confers on gibbon PKR greatly increased resistance to K3L (Fig. 2a, row 3). These findings reveal that even a single change in PKR at the common interface with substrate and mimic has the capacity to reverse a 'susceptibility' phenotype.

A second determinant, not in helix αG, explains the resistance of orangutan PKR to K3L. When we tested the αG configuration (S-A-K) of the 'resistant' orangutan *PKR* allele (Fig. 1c) in the gibbon backbone, this S-A-K allele was still quite susceptible (Fig. 2a, row 5). To identify the source of resistance of orangutan PKR, we tested chimaeras between orangutan and gibbon PKR and found that a region in the kinase domain containing helices αD and αE from orangutan PKR greatly increased the resistance of gibbon PKR to K3L (data not shown). When we tested individual substitutions in this region, we found that the F394L substitution of the αE helix conferred gibbon PKR with resistance against K3L (Fig. 2c). Importantly, the opposite L394F substitution greatly reduced resistance in orangutan PKR (Fig. 2c). Unlike helix αG, helix αE discrimination seems to be independent of PKR contact with its substrate because it is positioned away from the eIF2α interface (Fig. 2d)[15]. In addition, positive selection in helix αD suggested that this region could contribute to escaping mimicry, either directly or by virtue of co-evolution between helices αD and αG (Supplementary Table 9)[25]. However, we did not find functional evidence for the involvement of αD in resisting K3L over the evolutionary timeframe that we examined for this particular mimic (Supplementary Fig. 4). Therefore, susceptible gibbon *PKR* alleles can gain resistance to vaccinia K3L by single substitutions in either the αG helix or the αE helix (Fig. 2e), increasing the chances of escaping mimicry.

Our analyses suggested that human PKR contained residues associated with increased resistance to K3L from both αG and αE helices. Indeed, we found that a human *PKR* allele carrying 'susceptible' mutations in both its αE (L394F) and αG (F489Y/S492A) helices loses wild-type resistance to K3L (Fig. 3a, row 5). We tested all combinations of resistant and susceptible substitutions at positions 394 (helix αE), 489 and 492 (helix αG) in human PKR and found that six out of eight combinations of human *PKR* alleles resist K3L. The two exceptions are F-Y-A (described above) and F-F-A (Fig. 3a, row 4), which is only slightly more resistant than F-Y-A to K3L, revealing a weak effect associated with the positively selected residue at position 489. Although the human and gibbon PKR backbones bear similar outcomes at all positions (Fig. 3b), the 'susceptible' human alleles still seem more resistant than the 'susceptible' gibbon alleles to vaccinia K3L, hinting at an additional K3L resistance determinant in the human PKR sequence (data not shown).

One of the most notable findings from testing the 'susceptible' and 'resistant' PKR variants was that helices αE and αG had distinct means of defeating K3L. Leu 394 resisted K3L regardless of whether human, gibbon or orangutan PKR had a 'susceptible' αG helix (Fig. 2c and Supplementary Fig. 5). The mutational profile of the αE and αG helices is therefore not strictly independent, because helix αE masks αG in terms of K3L resistance. Only when helix αE is 'susceptible' does the configuration of αG matter. Residue 394 of helix αE toggles exclusively between leucine and phenylalanine at a much lower rate than residues of helix αG, not only in primates but also among mammals in general (Supplementary Fig. 6). Our finding that Leu 394 confers overriding resistance to vaccinia K3L strongly suggests that toggling can unmask potentially adaptive substitutions in the rapidly evolving αG helix. The fact that Phe 394 is fixed in numerous species, including the New World monkeys we sampled, suggests that phenylalanine rather than leucine might confer resistance against substrate mimics different from the two we tested in this study. Therefore, toggling at position 394 reveals how a single substitution, in combination with positive selection in helix αG, might effectively increase the adaptive space that PKR can explore, greatly increasing the odds of defeating substrate mimics.

Positive selection seems to be a major evolutionary driver of many host–pathogen interactions[11,18,26]. Strong positive selection seen in both primate PKR and poxvirus K3L, and the presence of substrate

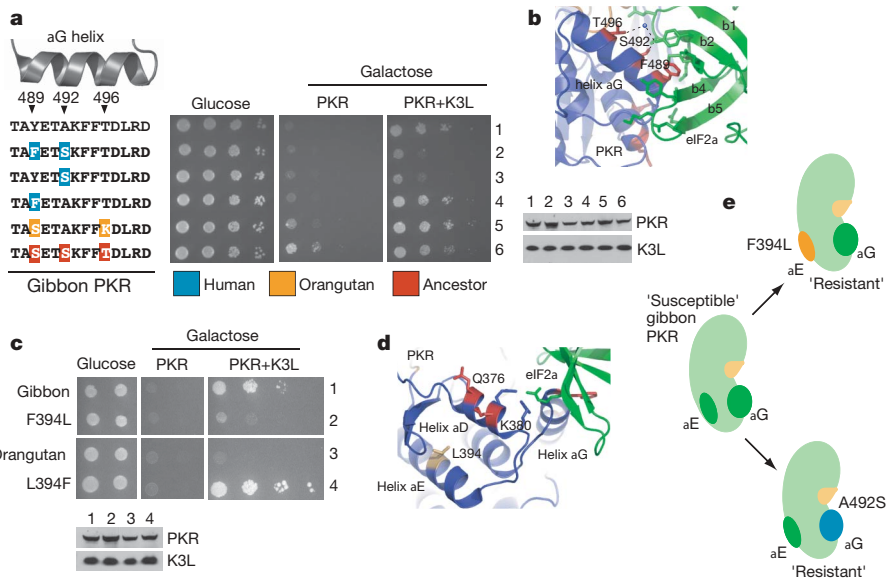

Figure 2 | Distinct surfaces of the PKR kinase domain are crucial to K3L resistance. **a**, Plasmids encoding gibbon *PKR* alleles with substitutions in the αG helix were introduced into yeast strains HM3 (eIF2α alone) and HM1 (eIF2α and K3L). Tenfold serial dilutions of transformants are shown. A corresponding immunoblot analysis is also shown with antibodies against PKR (top) and K3L (bottom). **b**, A ribbon representation of the PKR–eIF2α complex, highlighting the association of side chains of residues under positive selection with side chains of eIF2α. Phe 489, Ser 492 and Thr 496 form a face of the αG helix directly interacting with eIF2α (ref. 15). **c**, Plasmids encoding gibbon and orangutan *PKR* alleles with substitutions in the αE helix were introduced into yeast strains HM3 and HM1. Tenfold serial dilutions of transformants are shown, along with a corresponding immunoblot analysis. **d**, Residues under positive selection (Gln 376 and Lys 380) and residue Leu 394 from a ribbon representation of human PKR and eIF2α are shown[15]. **e**, Diagram showing that single substitutions in either the αE or αG helices can confer resistance against vaccinia K3L to gibbon PKR.

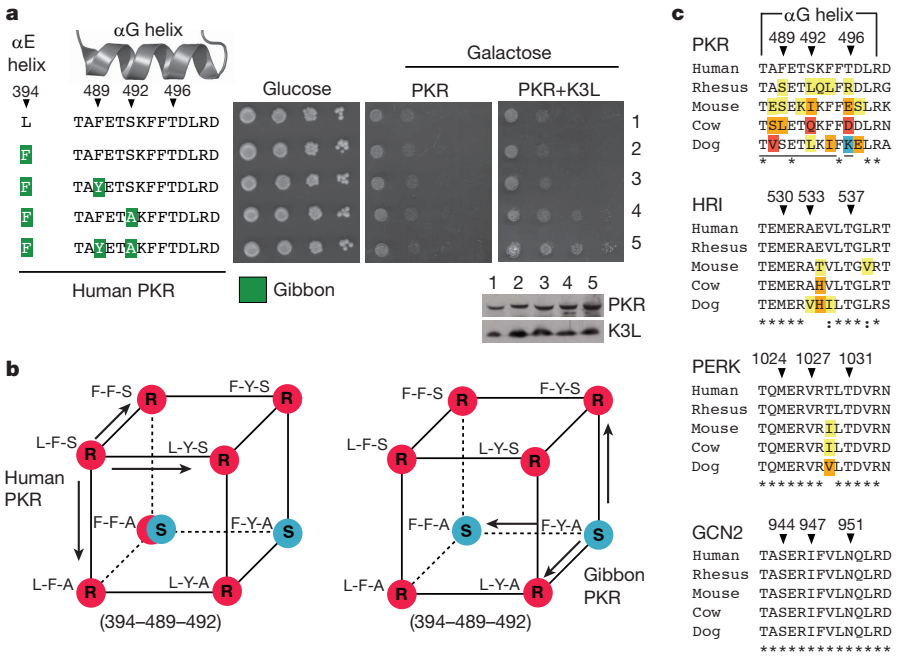

Figure 3 | PKR chimaeras reveal masking of K3L sensitivity by Leu 394. **a**, Tenfold serial dilutions of transformants expressing alleles of human *PKR* with combinations of substitutions in the αE and αG helices are shown, along with a corresponding immunoblot analysis. **b**, Phenotype 'cubes' summarizing the K3L susceptibility of alleles with all combinations of substitutions between human and gibbon PKR at positions 394, 489 and 492 from Figs 2a and 3a and Supplementary Fig. 5. Red and blue dots indicate resistance and sensitivity to K3L, respectively. With the exception of F-F-A, which shows some measure of resistance to K3L in the human background (indicated by the red crescent), each set of substitutions has similar phenotypes in the human and gibbon backgrounds. Each single substitution in wild-type human PKR results in a variant still resistant to K3L, whereas in two of three cases gibbon PKR becomes resistant (indicated by arrows). **c**, Sequence alignments of the αG helix for each member of the eIF2α kinase family (PKR, haem-regulated inhibitor (HRI), PKR-like ER kinase (PERK) and GCN2) from several mammals highlights the conservation of this region compared with the rapid evolution of PKR (black arrowheads indicate residues of the αG helix under positive selection in PKR). The frequency of substitutions in the panel at each position is indicated by a colour code (yellow for a single substitution, orange for a second, red for a third, and blue for a fourth), with the human sequence as a reference. Residues making contacts with eIF2α are indicated with lines below the PKR alignment.

mimics in unrelated viruses[27], clearly indicates that both host and viral genomes have been under intense pressure to gain advantages in these ancient and continuing evolutionary battles. The positive selection we observed in primate PKR is likely to reflect selection driven by ancient viruses with K3L-like factors that strongly influenced susceptibility to present-day mimics. For example, positive selection in the gibbon lineage driven by ancient mimics may have left gibbon PKR susceptible to vaccinia K3L. Similar trade-offs have been observed for variants of antiviral proteins under strong positive selection that might have defeated ancient retroviruses but are currently susceptible to HIV-1 (ref. 19).

Mimicry adds a layer of complexity to host–pathogen interfaces. Because PKR must distinguish an essentially unchanging substrate from rapidly evolving mimics such as K3L, it is surprising that most present-day hominoid species are resistant to vaccinia K3L (Fig. 1c). Our studies reveal evolutionary mechanisms that might allow host genes such as PKR to stave off mimicry. This strategy involves not only positive selection but also multiple discrimination interfaces (αE and αG helices) and a combinatorial outcome of resistance or susceptibility based on these surfaces, which together can increase discrimination against rapidly evolving mimics.

PKR seems well suited for molecular arms races against mimics because of a striking level of evolutionary flexibility. Because the biochemical activity of PKR depends on recognition of an unchanging substrate, strong purifying selection at the interaction interface would be expected. Indeed, other members of the eIF2α kinase family, which do not primarily serve antiviral functions and are not known to encounter viral mimicry directly, have highly conserved αG helices (Fig. 3c) and evolve under purifying selection ($dN < dS$; Supplementary Fig. 1). Despite extensive amino-acid diversity in helix αG, variants of PKR retain the ability to recognize eIF2α. The contrasting evolutionary trajectories of helix αG in the family of eIF2α kinases suggests that host factors challenged by mimics, such as PKR, rely on a high degree of flexibility to escape mimicry. We speculate that substantial selective pressures for distinguishing substrate mimics may even result in substitutions causing a decrease in substrate recognition until potential compensatory mutations might arise. Consistent with this situation was our finding that introducing an ancestral helix αG or one from orangutan into PKR from gibbon resulted in slightly compromised substrate recognition (Fig. 2a, middle, rows 5 and 6; also see Supplementary Fig. 7, middle), yet full substrate recognition was restored for helix αG from orangutan in the context of the whole protein (Fig. 1c, middle, orangutan). Compromising one function to explore a greater adaptive landscape for another function is probably a theme for genetic gains of functional novelty[28,29]. Because contending with viral mimicry can be essential for combating infectious disease, compromises to components of key cellular processes targeted by mimics[1–5,30] might be a 'hidden' evolutionary cost of such high-stakes genetic conflicts.

METHODS SUMMARY

Primate *PKR* cDNA was amplified, cloned, and sequenced from a panel of hominoids, as well as from Old World and New World monkeys. Poxvirus *K3L* sequences were retrieved from the Poxvirus Bioinformatics Resource Center (http://www.poxvirus.org). DNA sequences from each panel were aligned and used for phylogenetic and evolutionary analysis with the PAML[13] and HyPhy software packages. Structure observations of PKR were made with data coordinates from the Protein Databank (http://www.pdb.org; IDs 2A1A and 2A19) and MacPyMol software.

Variants of *PKR* and *K3L* were cloned into yeast vectors, and gene expression was driven in transformed yeast strains under a galactose-induced promoter. Yeast growth was monitored in serial-dilution series of transformants on plates containing selective medium and galactose as a carbon source. Western blots with

antibodies raised against PKR, K3L and the haemagglutinin (HA) epitope were performed to determine protein levels for yeast strains used in growth assays.

For virus infection assays, human, orangutan and white-cheeked gibbon fibroblasts were infected with 0.001 plaque-forming units per cell of wild-type or ΔK3L vaccinia virus (Copenhagen strain) for 1 h. Virus production was assessed 72 h after infection by titring cell lysates.

Full Methods and any associated references are available in the online version of the paper at www.nature.com/nature.

Received 19 August; accepted 8 October 2008.
Published online 30 November 2008.

1. Murphy, P. M. Molecular mimicry and the generation of host defense protein diversity. *Cell* **72,** 823–826 (1993).
2. Angot, A., Vergunst, A., Genin, S. & Peeters, N. Exploitation of eukaryotic ubiquitin signaling pathways by effectors translocated by bacterial type III and type IV secretion systems. *PLoS Pathog.* **3,** e3 (2007).
3. Benedict, C. A., Norris, P. S. & Ware, C. F. To kill or be killed: viral evasion of apoptosis. *Nature Immunol.* **3,** 1013–1018 (2002).
4. Izard, T., Tran Van Nhieu, G. & Bois, P. R. *Shigella* applies molecular mimicry to subvert vinculin and invade host cells. *J. Cell Biol.* **175,** 465–475 (2006).
5. Stebbins, C. E. & Galan, J. E. Structural mimicry in bacterial virulence. *Nature* **412,** 701–705 (2001).
6. Alcami, A. Viral mimicry of cytokines, chemokines and their receptors. *Nature Rev. Immunol.* **3,** 36–50 (2003).
7. Finlay, B. B. & McFadden, G. Anti-immunology: evasion of the host immune system by bacterial and viral pathogens. *Cell* **124,** 767–782 (2006).
8. Meurs, E. *et al.* Molecular cloning and characterization of the human double-stranded RNA-activated protein kinase induced by interferon. *Cell* **62,** 379–390 (1990).
9. Dever, T. E., Dar, A. C. & Sicheri, F. in *Translational Control in Biology and Medicine* (eds Mathews, M. B., Sonenberg, N. & Hershey, J. W. B.) 319–344 (Cold Spring Harbor Laboratory Press, 2007).
10. Langland, J. O., Cameron, J. M., Heck, M. C., Jancovich, J. K. & Jacobs, B. L. Inhibition of PKR by RNA and DNA viruses. *Virus Res.* **119,** 100–110 (2006).
11. Sawyer, S. L., Emerman, M. & Malik, H. S. Ancient adaptive evolution of the primate antiviral DNA-editing enzyme APOBEC3G. *PLoS Biol.* **2,** E275 (2004).
12. Nielsen, R. *et al.* A scan for positively selected genes in the genomes of humans and chimpanzees. *PLoS Biol.* **3,** e170 (2005).
13. Yang, Z. PAML 4: phylogenetic analysis by maximum likelihood. *Mol. Biol. Evol.* **24,** 1586–1591 (2007).
14. Scheffler, K., Martin, D. P. & Seoighe, C. Robust inference of positive selection from recombining coding sequences. *Bioinformatics* **22,** 2493–2499 (2006).
15. Dar, A. C., Dever, T. E. & Sicheri, F. Higher-order substrate recognition of eIF2α by the RNA-dependent protein kinase PKR. *Cell* **122,** 887–900 (2005).
16. Li, Y. *et al.* On the origin of smallpox: correlating variola phylogenics with historical smallpox records. *Proc. Natl Acad. Sci. USA* **104,** 15787–15792 (2007).
17. Babkin, I. V. & Shchelkunov, S. N. The time scale in poxvirus evolution. [In Russian.] *Mol. Biol. (Mosk.)* **40,** 20–24 (2006).
18. Sawyer, S. L., Wu, L. I., Emerman, M. & Malik, H. S. Positive selection of primate TRIM5α identifies a critical species-specific retroviral restriction domain. *Proc. Natl Acad. Sci. USA* **102,** 2832–2837 (2005).
19. Kaiser, S. M., Malik, H. S. & Emerman, M. Restriction of an extinct retrovirus by the human TRIM5α antiviral protein. *Science* **316,** 1756–1758 (2007).
20. Chong, K. L. *et al.* Human p68 kinase exhibits growth suppression in yeast and homology to the translational regulator GCN2. *EMBO J.* **11,** 1553–1562 (1992).
21. Dey, M. *et al.* Mechanistic link between PKR dimerization, autophosphorylation, and eIF2α substrate recognition. *Cell* **122,** 901–913 (2005).
22. Dever, T. E. *et al.* Mammalian eukaryotic initiation factor 2α kinases functionally substitute for GCN2 protein kinase in the GCN4 translational control mechanism of yeast. *Proc. Natl Acad. Sci. USA* **90,** 4616–4620 (1993).
23. Kawagishi-Kobayashi, M., Silverman, J. B., Ung, T. L. & Dever, T. E. Regulation of the protein kinase PKR by the vaccinia virus pseudosubstrate inhibitor K3L is dependent on residues conserved between the K3L protein and the PKR substrate eIF2alpha. *Mol. Cell. Biol.* **17,** 4146–4158 (1997).
24. Langland, J. O. & Jacobs, B. L. The role of the PKR-inhibitory genes, E3L and K3L, in determining vaccinia virus host range. *Virology* **299,** 133–141 (2002).
25. Poon, A. F., Lewis, F. I., Pond, S. L. & Frost, S. D. An evolutionary-network model reveals stratified interactions in the V3 loop of the HIV-1 envelope. *PLOS Comput. Biol.* **3,** e231 (2007).
26. Kerns, J. A., Emerman, M. & Malik, H. S. Positive selection and increased antiviral activity associated with the PARP-containing isoform of human zinc-finger antiviral protein. *PLoS Genet.* **4,** e21 (2008).
27. Essbauer, S., Bremont, M. & Ahne, W. Comparison of the eIF-2α homologous proteins of seven ranaviruses (Iridoviridae). *Virus Genes* **23,** 347–359 (2001).
28. Ortlund, E. A., Bridgham, J. T., Redinbo, M. R. & Thornton, J. W. Crystal structure of an ancient protein: evolution by conformational epistasis. *Science* **317,** 1544–1548 (2007).
29. Dean, A. M. & Thornton, J. W. Mechanistic approaches to the study of evolution: the functional synthesis. *Nature Rev. Genet.* **8,** 675–688 (2007).
30. Sawyer, S. L. & Malik, H. S. Positive selection of yeast nonhomologous end-joining genes and a retrotransposon conflict hypothesis. *Proc. Natl Acad. Sci. USA* **103,** 17614–17619 (2006).

Supplementary Information is linked to the online version of the paper at www.nature.com/nature.

Acknowledgements We thank T. Dever for yeast strains and advice; J. Tartaglia and B. Jacobs for valuable reagents; and S. Biggins and S. Furuyama for yeast expression plasmids and advice, and M. Emerman, S. Henikoff, S. Biggins, A. Turkewitz, D. Gottschling, D. Koshland, E. Smith, J. Kerns, S. Sawyer and D. Vermaak for comments and suggestions. We are supported by NIH grant AI026672 (A.P.G.) and a Searle Scholar and Burroughs Wellcome Investigator Award (H.S.M.). N.C.E. is an Ellison Medical Foundation Fellow of the Life Sciences Research Foundation.

Author Contributions N.C.E. and H.S.M. designed the study. N.C.E. performed the evolutionary analysis and yeast growth assays. S.J.C. and A.P.G. designed and performed the vaccinia infection experiments. N.C.E. and H.S.M. wrote the paper. All authors discussed and edited the manuscript.

Author Information Sequences of PKR have been deposited in Genbank under accession numbers EU733254–EU733271 and FJ374685. Reprints and permissions information is available at www.nature.com/reprints. Correspondence and requests for materials should be addressed to H.S.M. (hsmalik@fhcrc.org).

METHODS

Primate genomic sources. Total RNA was obtained (RNeasy kit; Qiagen) from the following cell lines from the Coriell Cell Repositories except where otherwise noted: *Homo sapiens* (human; primary human foreskin fibroblasts), *Pan troglodytes* (chimpanzee; AG06939), *Pan paniscus* (bonobo; AG05253), *Gorilla gorilla* (western lowland gorilla; AG05251), *Pongo pygmaeus pygmaeus* (Bornean orangutan; AG05252), *Hylobates agilis albibarbis* (agile gibbon; PR00773), *Hylobates leucogenys* (white-cheeked gibbon; PR01037), *Hylobates syndactylus* (island siamang; PR00722), *Cercocebus atys* (sooty mangabey; gift from C. Apetrei), *Macaca mulatta* (rhesus monkey; TF-1 cells), *Miopithecus talapoin talapoin* (talapoin monkey; PR00716), *Erythrocebus patas* (patas monkey; AG06116), *Cercopithecus aethiops* (African green monkey; COS cells), *Trachypithecus francoisi* (Francois' leaf monkey; PR01099), *Colobus guereza* (colobus monkey; PR00980), *Lagothrix lagotricha* (common woolly monkey; AG05356), *Ateles geoffroyi* (black-handed spider monkey; AG05352), *Callicebus moloch* (dusky titi; AG06115), *Aotus trivirgatus* (owl monkey; CRL-1556; American Type Culture Collection) and *Saguinus labiatus* (red-chested mustached tamarin; AG05308).

cDNA cloning and sequences. RNA (50 ng) from each primate was used for RT–PCR (SuperScript III; Invitrogen) with primers listed in Supplementary Table 10. PCR products were TA-cloned into pCR2.1 (Invitrogen) and sequenced from three different clones. The human PKR variant we cloned was identical in sequence to the GenBank entry for this gene (NM002759). The *PKR* cDNA sequence from *Callithrix jacchus* (common marmoset) was obtained by means of Blat searches of the UCSC Genome browser with PKR sequences from other New World monkeys to aid in identifying exon/intron boundaries. Other mammalian sequences of PKR, HRI, PERK and GCN2 were obtained from GenBank or by means of Blat searches of the UCSC Genome browser (http://genome.ucsc.edu). Vaccinia (Copenhagen) and variola (major) and other poxvirus K3L sequences were obtained from the Poxvirus Bioinformatics Resource Center (http://www.poxvirus.org).

PKR variants were ligated into 2-μm (pSB819; URA) and CEN (pSB146; URA) yeast *pGAL* expression plasmids by means of *Xho*I and *Not*I sites introduced into PKR primers. K3L or amino-terminal HA-epitope-tagged K3L from vaccinia virus (Copenhagen strain) was amplified by PCR, TA cloned, sequenced for accuracy, and ligated by means of *Xho*I and *Not*I sites into an integrating (pSB305; LEU) yeast expression plasmid into which a galactose promoter was also introduced. Variola major K3L sequence was synthesized by standard methods (CelTek Genes) and subcloned in the same manner as K3L from vaccinia. For comparisons of helix αE the following mammalian sequences of PKR were obtained from GenBank: *Mus musculus* (mouse; NP_035293), *Rattus norvegicus* (rat, NP_062208), *Oryctolagus cuniculus* (rabbit, NP_001075682), *Canis lupus familiaris* (dog, NP_001041600), *Equus caballus* (horse, XP_001917876), *Bos taurus* (cow, NP_835210) and *Sus scrofa* (pig, NP_999484).

Evolutionary analysis and structure observations. DNA sequences were aligned by using ClustalW with small indels trimmed on the basis of amino-acid comparisons (Supplementary Data). The generally accepted primate phylogeny (Fig. 1a) was used for evolutionary analysis, although a neighbour-joining tree generated from the alignment of PKR placed gorilla and owl monkey at different nodes (Supplementary Fig. 8). Parallel analysis with the PKR tree did not alter any results significantly (data not shown). Pairwise d*N*/d*S* analysis of eIF2α kinases, eIF2α and K3L were performed with *K*-estimator software[31]. Maximum-likelihood analysis of the larger PKR data set was performed with codeml of the PAML software package[13]. A free-ratio model allowing d*N*/d*S* variation along different branches of the phylogeny was employed to calculate d*N*/d*S* values between lineages. Two-ratio tests were performed with likelihood models comparing all branches fixed at d*N*/d*S* = 1 or an average d*N*/d*S* value from the whole tree applied to each branch to varying d*N*/d*S* values according to branch. Complementary analysis grouping lineages according to d*N*/d*S* values with multi-model inference (HyPhy software)[32] was also applied to the data set. We uncovered support for one recombination breakpoint in the data set by using the GARD program (HyPhy software; see Supplementary Table 5).

To detect selection in PKR, the multiple alignment was fitted to either F3x4 or F61 codon frequency models. Likelihood ratio tests (LRTs) were performed by comparing the following site-specific models (*NS* sites): M1 (neutral) with M2 (selection), M7 (neutral, β distribution of d*N*/d*S* < 1) with M8 (selection, beta distribution, d*N*/d*S* > 1 allowed), and M8a (neutral, with class of sites at d*N*/d*S* = 1) with M8. Similar LRTs that also account for synonymous rate variation and recombination (PARRIS; HyPhy software) were performed. Co-evolution analysis between PKR residues was also performed (Spidermonkey/BGM; HyPhy software).

PAML analysis identified sets of amino acids with high posterior probabilities (more than 0.90) for positive selection by a Bayesian approach. Similar analysis identified amino acids under positive selection with the LRTs implemented in the SLAC, FEL and REL programs (HyPhy software). Amino acids under positive selection in the kinase domain were examined using the PKR–eIF2α structure data coordinates available in the Protein Databank (PDB IDs 2A1A and 2A19; http://www.pdb.org)[15] and MacPyMol software[33].

Yeast strains and growth assays. Standard techniques were used for culturing and transforming yeast strains[34]. Strain H2557 was provided by T. Dever[21] and modified by integrating K3L or HA–K3L under the *gal* promoter at the *leu2* locus. Integration of *K3L* alleles in the resulting strains HM1 and HM2 were confirmed by PCR with primers flanking the *leu2* locus. HM3 was generated from H2557 by transforming empty pSB305 linearized with *Eco*RV. Genotypes of these strains are shown in Supplementary Table 11.

Strains HM1, HM2, HM3, HM4 and J223 (S51A allele of eIF2α; provided by T. Dever)[21] were transformed with PKR variants in 2-μm plasmid pSB819 for growth assays. Transformants were grown in YC-leu-ura medium (yeast complete minimal medium with amino acids) containing 2% glucose, then washed and plated in dilution series of D_{600} = 3.0, 0.3, 0.03, 0.003 with the use of a bacterial replicator (Aladin Enterprises) on YC-leu-ura medium containing either 2% glucose or 2% galactose and grown for 6 days (the human chimaera set shown in Fig. 3 and Supplementary Fig. 5 was grown for 10 days). Growth assays with PKR variants expressed from CEN plasmid pSB146 yielded consistent results (data not shown).

Western blotting. Transformants were grown to saturation in YC-leu-ura medium with 2% glucose, then washed and diluted 1:50 in YC-leu-ura medium with 2% galactose and grown for 15 h. Whole-cell lysates were prepared[35] and resolved by SDS–PAGE (12% Tris-glycine gel; Invitrogen). Proteins were transferred to nitrocellulose membranes and detected with anti-PKR antibody B-10 (1:1,000 dilution; Santa Cruz Biotechnology), anti-HA.11 (1:1,000; Covance) or a monoclonal antibody against K3L (1:2,000; a gift from J. Tartaglia).

Primate PKR infection assays. Human, orangutan and white-cheeked gibbon fibroblasts were maintained in Eagle's minimal essential medium with Earle's salts and non-essential amino acids, supplemented with 10% fetal bovine serum (Gibco), penicillin–streptomycin (100 U ml^{-1}) and 2 mM L-glutamine. Vaccinia virus Copenhagen strain (VC2)[36] and VVΔK3L (ref. 37), both obtained from B. Jacobs, were propagated and titred in BSC_{40} cells. Growth and titration of VV stocks were performed essentially as described[38], except that virus stocks were partly purified after cell lysis by centrifugation through a 36% sucrose cushion before resuspension in 1 mM Tris-HCl pH 9.0, division into aliquot, and storage at −70 °C.

Human, orangutan and gibbon fibroblasts in triplicate wells were infected with VC2 or VVΔK3L at 0.001 plaque-forming units per cell for 1 h, washed twice, and re-fed with medium. At 72 h after infection the infected cells were collected and freeze-thawed three times, and the resulting lysates were titred on BSC_{40} cells[39].

31. Comeron, J. M. K-Estimator: calculation of the number of nucleotide substitutions per site and the confidence intervals. *Bioinformatics* **15,** 763–764 (1999).
32. Pond, S. L. & Frost, S. D. A genetic algorithm approach to detecting lineage-specific variation in selection pressure. *Mol. Biol. Evol.* **22,** 478–485 (2005).
33. DeLano, W. L. *The PyMOL User's Manual* (DeLano Scientific, 2004).
34. Gietz, R. D. & Woods, R. A. Transformation of yeast by lithium acetate/single-stranded carrier DNA/polyethylene glycol method. *Methods Enzymol.* **350,** 87–96 (2002).
35. Kushnirov, V. V. Rapid and reliable protein extraction from yeast. *Yeast* **16,** 857–860 (2000).
36. Tartaglia, J. *et al.* Highly attenuated poxvirus vectors. *AIDS Res. Hum. Retroviruses* **8,** 1445–1447 (1992).
37. Beattie, E., Tartaglia, J. & Paoletti, E. Vaccinia virus-encoded eIF-2α homolog abrogates the antiviral effect of interferon. *Virology* **183,** 419–422 (1991).
38. Earl, P. L., Cooper, N., Wyatt, L. S., Moss, B. & Carroll, M. W. Preparation of cell cultures and vaccinia virus stocks. *Curr. Protocols Protein Sci.* 5, Unit 5.12 doi:10.1002/0471140864.ps0512s13 (2001).
39. Dar, A. C. & Sicheri, F. X-ray crystal structure and functional analysis of vaccinia virus K3L reveals molecular determinants for PKR subversion and substrate recognition. *Mol. Cell* **10,** 295–305 (2002).